Journal of Crystal Growth 90 (1988) 231–244
North-Holland, Amsterdam

CRYSTALLOGRAPHY OF RIBOSOMAL PARTICLES

A. YONATH *, F. FROLOW and M. SHOHAM

Department of Structural Chemistry, Weizmann Institute, Rehovot, Israel

J. MÜSSIG, I. MAKOWSKI and C. GLOTZ

Max-Planck-Institute for Molecular Genetics, D-1000 Berlin (West), Germany

W. JAHN

Max-Planck-Institute for Medical Research, D-6900 Heidelberg, Fed. Rep. of Germany

and

S. WEINSTEIN ** and H.G. WITTMANN

Max-Planck-Institute for Molecular Genetics, D-1000 Berlin (West), Germany

Received 12 August 1987; manuscript received in final form 24 September 1987

Several forms of three-dimensional crystals and two-dimensional sheets of intact ribosomes and their subunits have been obtained as a result of: (a) an extensive systematic investigation of the parameters involved in crystallization, (b) a development of an experimental procedure for controlling the volumes of the crystallization droplets, (c) a study of the nucleation process, and (d) introducing a delicate seeding procedure coupled with variations in the ratios of mono- and divalent ions in the crystallization medium. In all cases only biologically active particles could be crystallized, and the crystalline material retains its integrity and activity. Crystallographic data have been collected from crystals of 50S ribosomal subunits, using synchrotron radiation at temperatures between +19 and −180 °C. Although at 4 °C the higher resolution reflections decay within minutes in the synchrotron beam, at cryo-temperature there was hardly any radiation damage, and a complete set of data to about 6 Å resolution could be collected from a single crystal. Heavy-atom clusters were used for soaking as well as for specific binding to the surface of the ribosomal subunits prior to crystallization. The 50S ribosomal subunits from a mutant of *B. stearothermophilus* which lacks the ribosomal protein BL11 crystallize isomorphously with in the native ones. Models, aimed to be used for low resolution phasing, have been reconstructed from two-dimensional sheets of 70S ribosomes and 50S subunits at 47 and 30 Å, respectively. These models show the overall structure of these particles, the contact areas between the large and small subunits, the space where protein synthesis might take place and a tunnel which may provide the path for the nascent protein chain.

1. Introduction

Ribosomes are the cell organelles on which protein biosynthesis takes place in all organisms. They consist of two different subunits which associate upon initiation of the biosynthesis process. Each ribosomal subunit is a defined assembly of proteins and ribonucleic acid chains. A typical bacterial ribosome has a molecular weight of 2.300.000 daltons. Its large (50S) subunit is of 1.600.000 daltons and consists of 32–35 different proteins and 2 RNA chains. The small subunit (30S) is of 700.000 daltons and contains about 20 proteins and 1 RNA chain. During the last two decades extensive information has been accumulated about the function and the chemical, physical, biological and genetic properties of ribosomes [1–4]. This has shed light on basic points in the process of protein biosynthesis,

* Also at: Max-Planck-Research Unit for Structural Molecular Biology, D-2000 Hamburg, Fed. Rep. of Germany.

** Also at: Department of Structural Chemistry, Weizmann Institute, Rehovot, Israel.

though the understanding of the detailed mechanism is still limited by the lack of a molecular model. To this end, we undertook crystallographic studies.

As object for crystallographic studies, ribosomal particles are of enormous size with no internal symmetry. Furthermore, they are instable and flexible. Therefore, their crystallization seem to be a formidable task. In spite of this, as a result of an intensive systematic exploration of crystallization conditions and development of an innovative experimental technique for fine control of the volume of the crystallization mixture [5], procedures for in vitro growth of crystals of intact ribosomal particles have been developed. These procedures, combined with sophisticated seeding proved to be suitable for the reproducible production of ordered three-dimensional crystals and two-dimensional sheets of whole 70S ribosomes [6–8] as well as of small and large ribosomal subunits [8–22].

There is a strong correlation between crystallizability and biological activity. Inactive ribosomal particles could not be crystallized. Moreover, in all cases, the crystalline material retains its biological activity for long periods in spite of the natural tendency of ribosomes to disintegrate and in contrast to the short life time of isolated ribosomes in solution. Preservation of activity in the crystalline state accords well with the hypothesis than when external conditions (e.g. a cold shock, hibernation, etc.) demand prolonged storage of potentially active ribosomes in living organisms, temporary periodic organization occurs in vivo.

The best crystals are those of the large ribosomal subunits. Ordered three-dimensional crystals grow from virtually all preparations of active large (50S) ribosomal subunits of *Bacillus stearothermophilus* and of *Halobacterium marismortui*. However, due to the intricate nature of the particles, the exact conditions for the growth of well ordered crystals must still be slightly varied for each ribosomal preparation. Moreover, for each crystal form the quality of the crystals depends, in a manner not yet fully characterized, on the procedure used for preparation of the ribosomal subunits and on the strain of a given bacterial species.

In this manuscript we describe the procedures used for crystal growth as well as for the consequent crystallographic studies. We also show our results obtained by three-dimensional image reconstruction from two-dimensional sheets.

2. Experimental procedures

The growth of the different bacterial species, the production of their ribosomes, and the biological characterization are described in refs. [9,15]. The procedures used for crystal growth and the crystallographic studies are discussed in detail in refs. [5,9–13,15–20]. The exact growth conditions are given in the legends to the various figures. Two-dimensional sheets were grown according to refs. [7,8,21,22]. The image reconstruction studies are described in refs. [8,21]. Synchrotron radiation was used for all crystallographic studies at 19, 14, 4, −10, −20 and −180 °C [10–13,17–20]. For noncovalent binding of heavy-atoms, crystals were soaked in solutions of heavy-atom clusters (2mM–10mM) for 6–12 h, and washed in transfer solutions (fig. 6d) for 4–6 h.

Radioactive N-ethylmaleimide was reacted with ribosomal particles to determine the accessibility and the location of sulfhydryl groups in ribosomal proteins. A gold cluster and its radioactive derivative were prepared following basically a procedure described in ref. [23]. Functional groups were attached to this cluster for covalent binding to ribosomal particles through accessible sulfhydryl groups (S. Weinstein and W. Jahn, in preparation). The extent of binding of the gold cluster was determined by measuring the radioactivity associated with the 50S particles as well as by neutron activation (performed at Soreq Nuclear Research Laboratories, Israel). The proteins which bind the cluster and/or N-ethylmaleimide were identified by locating the radioactivity on two-dimensional gel electropherograms of the ribosomal proteins. The procedures will be published elsewhere in detail.

3. Results and discussion

3.1. Crystallographic studies

Crystals of whole (70S) ribosomes (refs. [6,13] and fig. 1), small (30S) ribosomal subunits (refs.

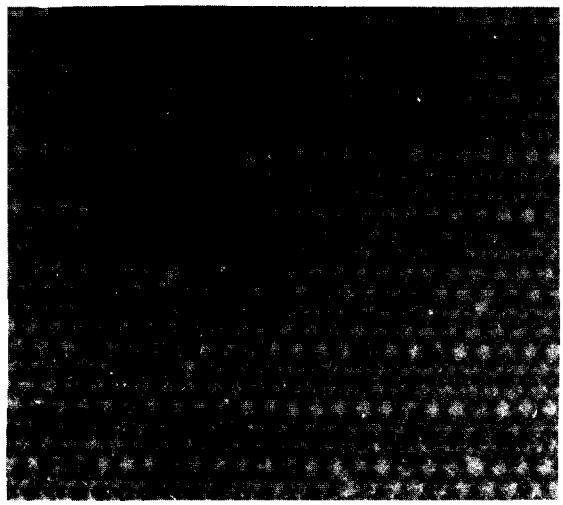

Fig. 1. Thin sections of epon (ERL 4206) embedded three-dimensional crystals of 70S ribosomes from *Thermus thermophilus* positively stained with 2% uranyl acetate. The crystals were grown from 15% methyl pentanediol at 4°C, pH 7.5, in hanging drops (bar = 1000 Å).

[13,19,20] and fig. 2) and large (50S) ribosomal subunits [9–20] have been obtained. Some are suitable for crystallographic studies in relatively high resolution, and are described below in detail.

3.1.1. 50S ribosomal particles from Bacillus stearothermophilus

Because ribosomes from eubacteria fall apart at high salt concentrations, at first volatile organic solvents had to be used as precipitants. A modified version of the standard hanging drop technique, using glass plates, was developed (ref. [5] and fig. 3). The crystallization droplets, which contained no precipitant or an extremely small quantity of it, were equilibrated with a reservoir containing the volatile precipitant. As a result of a comprehensive and intensive survey, the crystallization conditions for obtaining microcrystals have been determined. Attempts to increase the size of these crystals by a drastic slow-down of the crystallization process failed, since ribosomal particles from this source are unstable and may deteriorate before they are able to aggregate and form proper nucleation centers [24].

Growing crystals from volatile organic solvents imposes many technical difficulties in manipulating, data collection and heavy-atom derivatization. In fact, any handling of the crystals, such as removing or reorienting the crystals, or replacing the growth medium with a different solution, is detrimental for the crystals. Thus for this system, seeding was futile. However, reducing the size of the exposed surface of the crystallizing droplet led to the production of large crystals. This was achieved by growing crystals directly in X-ray capillaries (fig. 3).

Crystals of 50S subunits from the wild type and a mutant of *Bacillus stearothermophilus* have been grown at 4°C from mixtures of methanol and ethylene glycol (9–12) in X-ray capillaries. These may reach a length of 2.0 mm and a cross-section of 0.4 mm (fig. 4). Since most of the crystals growth with one of their faces adhering to the walls of the capillaries, it was possible to irradiate them without removing the original growth solution. Although the crystals tend to grow with their long axes parallel to the capillary axis, a fair number of them grow in different directions. Thus,

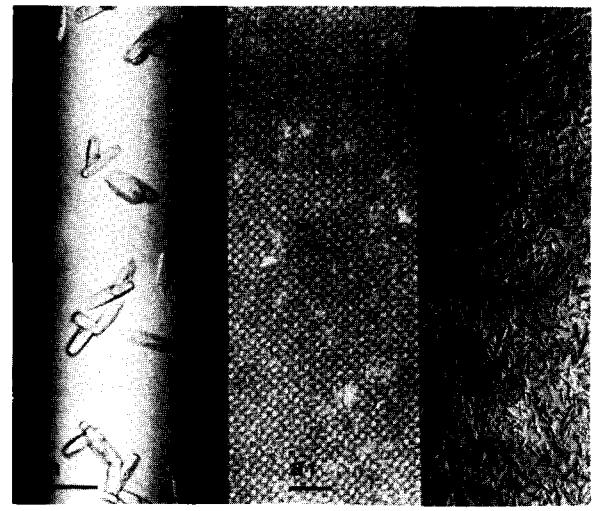

Fig. 2. Crystals of 30S subunits from (a) *Thermus thermophilus* grown in X-ray capillaries (ref. [5] and fig. 3) from a mixture of 20% ethyl butanol and 10% ethanol at pH 8.2 (bar = 0.2 mm) and (b) *H. marismortui*, grown from 5% polyethylene glycol in the presence of 2 M KCl, 0.5M ammonium chloride and 100mM magnesium chloride at pH 5.7 in hanging drops (bar = 0.1 mm). (a1) Electron micrograph of a thin section of an embedded crystal shown in (a), positively stained with 2% uranyl acetate (bar = 1000 Å).

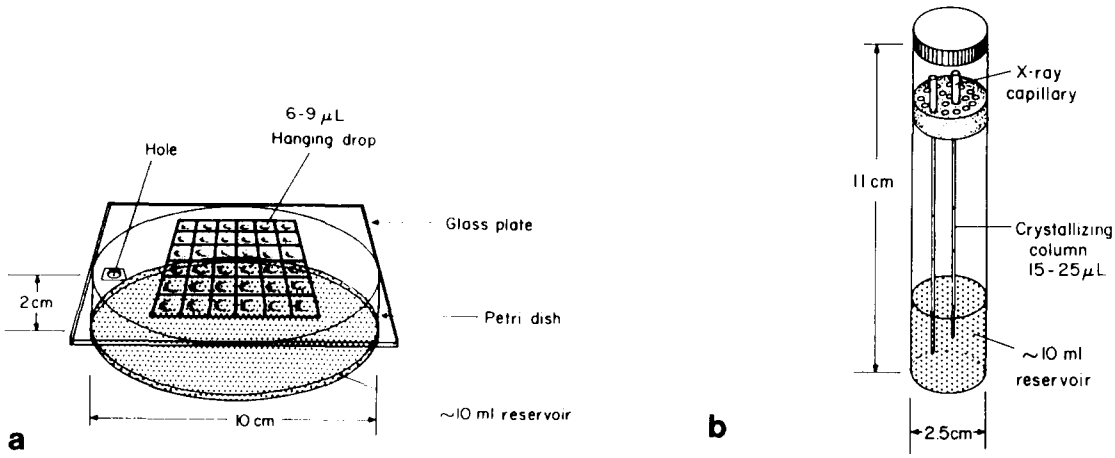

Fig. 3. (a) The crystallization system used for the initial survey in hanging drops. (b) The crystallization system used for production of large crystals, grown from mixtures of alcohols.

we were able to determine the unit cell constants and obtain diffraction patterns from all of the zones without manipulating the crystals. The crystals are loosely packed in a orthorhombic ($P2_12_12_1$) unit cell of $360 \times 680 \times 920$ Å. They diffract to 10–13 Å resolution at best (typically 15–18 Å). Although we often could obtain several X-ray photographs from a single crystal, the higher resolution reflections decay within 5–10 min in the synchrotron beam, as in the case of the crystals from ribosomal particles from halobacteria.

Oriented arcs and distinct spots, extending to 3.5 Å, with spacings similar to those measured from diffuse diffraction patterns of ribosome gels and extracted rRNA [25–27] have been detected on a few diffraction patterns of single crystals as well as on those of samples containing large numbers of microcrystals. For aligned crystals the average arc length was 60°. These patterns are similar to those observed for nucleosomes [28] and may arise from partial orientation of the nucleic acid component within the particle.

Recently we have succeeded to obtain a new crystal form from the 50S subunits of *B. stearothermophilus*. These crystals are grown in hanging drops using polyethylene glycol in the presence of the ions which are essential for maintaining the integrity of the particles in concentrations which are somewhat higher that commonly used for storage or for crystallization from alcohols [9]. The crystals are compactly packed, and preliminary X-ray diffraction patterns show periodic spacings of about 260, 320 and 700 Å.

3.1.2. 50S ribosomal subunits from Halobacterium marismortui

In contrast to ribosomal particles from eubacteria, halophilic ribosomal particles are stable and active at high salt concentrations. Thus, they can be crystallized from salts or other non-volatile compounds in biologically active state [15–17]. The growth solution mimics, to some extent, the natural environment within the halobacteria. Thus, potassium chloride, ammonium chloride and magnesium chloride are present in the mother liquor together with polyethylene glycol, the crystallization agent.

At first, microcrystals were obtained by vapor diffusion in hanging drops in solutions containing the above mentioned salts in high concentration. These microcrystals appeared within 1–2 days and were rather disordered. Better crystals were grown when the process of crystal growth was slowed down by using lower salt concentrations in the crystallization mixtures as well as in the reservoirs. In fact, the salt concentrations were reduced to the minimum needed for storage without activity loss [15]. For obtaining large and ordered crystals, advantage has been taken of the delicate equilibrium of mono- and divalent ions needed for the

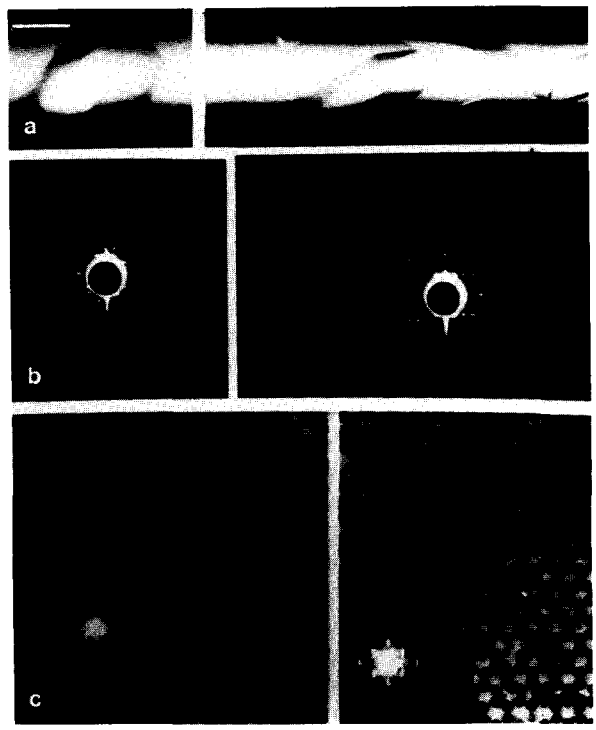

Fig. 4. (a) Crystals of the 50S ribosomal subunits from *B. stearothermophilus* grown in 0.5 mm X-ray capillaries by vapor diffusion at 4°C. Crystallization mixture of 20 μl 50S ribosomal subunits (10–20 mg/ml) in H–I buffer [9], 0.01M spermine, 1% methanol, 10 mM Hepes or glycine buffer, pH 8.4, was equilibrated with a reservoir of 12% methanol, 12% ethylene glycol, 0.5M NaCl, pH 8.4 (bar = 0.4 mm). (b) X-ray diffraction patterns from crystals similar to those shown in (a), obtained at −4°C with synchrotron radiation (A1 station at Chess/Cornell University operating at 5 GeV, current 30–40 mA) with 0.3 mm collimated X-ray beam with wave length of 1.55 Å, on a Huber precession camera equipped with a He path. Left: 1° rotation photograph of 0*kl* zone, 680×920 Å. Right: 0.4° rotation photograph of hk0 zone, 360×680 Å. (c) Electron micrographs of positively stained (2% uranyl acetate) thin sections of crystals similar to those shown in (a) that have been fixed in 0.2% glutaraldehyde and embedded in epon resin ERL 4206. Optical diffraction patterns are inserted. Left: Section approximately perpendicular to that shown on the right. Repeat distances measured from optical diffraction: 330×1050 Å. This corresponds to the *h*0*l* zone (360×920 Å) in the X-ray patterns (bar = 1000 Å). Right: Micrograph showing the characteristic open packing of this crystal form. The orthogonal choice of axes corresponds to the 680×920 Å zone observed in the X-ray diffraction patterns. Lattice spacing calculated from optical diffraction: 670×850 Å.

growth of halobacteria as well as of the major role played by the Mg^{2+} concentration in the crystallization of ribosomal particles. It was found earlier that three-dimensional crystals of 50S ribosomal particles from *B. stearothermophilus* grow in relatively low Mg^{2+} concentration, whereas the production of two-dimensional sheets requires a high Mg^{2+} concentration, at which growth of three-dimensional crystals is prohibited [14]. Similarly, for spontaneous crystal growth of 50S subunits from Halobacterium marismortui, the lower the Mg^{2+} concentration is, the thicker the crystals are. With these points in mind, a variation of the standard seeding procedure has been developed. Thin crystals of the 50S subunits from *Halobacterium marismortui*, grown spontaneously under the lowest possible Mg^{2+} concentration, were transferred to solutions in which the Mg^{2+} concentration was so low that the transferred crystals appeared to dissolve, but after about two weeks well ordered crystals were formed. These were about 10–20 fold thicker than the original seeds (fig. 6 and refs. [17,18]).

Orthorhombic crystals of the 50S subunits from *Halobacterium marismortui* grow as fragile thin plates with a maximum size of 0.6 × 0.6 × 0.2 mm. They diffract to a resolution of 5.5 Å at best, and have relatively small, densely packed unit cells ($C222_1$, 214 × 300 × 590 Å, fig. 7), in contrast to the "open" structure of the large crystals of *Bacillus stearothermophilus* (fig. 4). Although between −2 and 4°C up to 15 photographs can be taken from an individual crystal, the high resolution reflections appear only on the first 2–3 X-ray photographs. Hence, under these conditions over 260 crystals had to be irradiated in order to obtain a complete data set, and X-ray diffraction data were obtained from crystals which were aligned only visually, with a similar algorithm to that applied for rhino virus [29]. At cryo-temperature (i.e. −180°C), however, irradiated crystals hardly show radiation damage for days. Thus, for the first time, a full data set could be collected from a single crystal. Moreover, at cryo-temperature the life time of the crystals is long enough to allow preliminary X-ray diffraction experiments using rotating anodes as X-ray generators. Thus, basic parameters such as resolution, unit cell constants

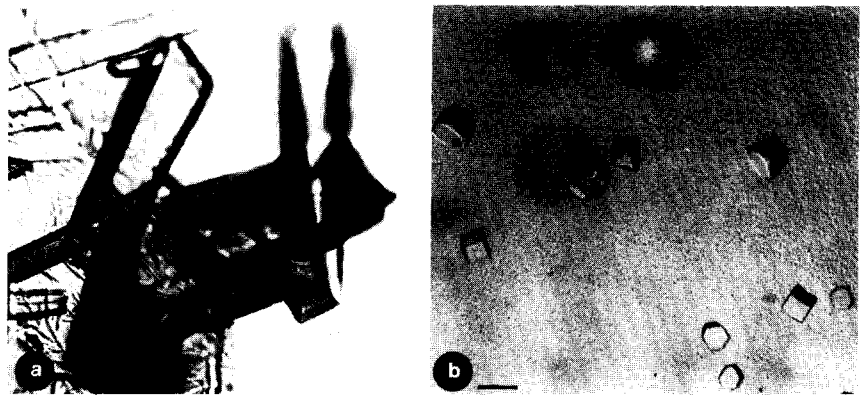

Fig. 5. Crystals of 50S ribosomal particles from *B. stearothermophilus* grown from polyethylene glycol at 4°C in hanging drops (bar = 0.1 mm). (a) Crystallization solution, at pH 6.6, of 2.5% polyethylene glycol, 0.2M KCl, 0.18M ammonium sulfate, 0.03M magnesium chloride and 50S particles in H–I buffers [9] was equilibrated with a reservoir of 0.5M KCl and all materials of the droplet. (b) Crystallization solution, at pH 6.4, of 2.5% polyethylene glycol, 0.02M ammonium sulfate, 0.02M magnesium chloride and 50S subunits in H–I buffer [9] was equilibrated with a reservoir of 0.15M ammonium sulfate together with all other materials in the droplet.

and isomorphism may be determined in the X-ray laboratories, and the progress of structure determination is expected to be less dependent on the availability of synchrotron radiation.

3.1.3. Nucleation

The process of crystal growth is initiated by nucleation. Although many biological molecules and complexes have been crystallized, little is known about the mechanism or nucleation. Theoretical models have been developed for the nucleation of crystals of small molecules [30,31]. Some data are available concerning the process of nucleation of crystals of biological systems. These are based on rather indirect evidence, such as monitoring aggregation under crystallization conditions by scattering techniques [32]. Because ribosomal particles are large enough to be detected by electron microscopy, crystals of ribosomal particles provide an excellent system for direct investigation of nucleation. The crystallization process was interrupted before the formation of mature crystals, and the crystallization medium was examined by electron microscopy. It was found that the first step in crystal growth is aggregation and that nucleation starts by a rearrangement within the aggregates [24].

3.1.4. Phase determination

The most common method in protein crystallography to derive phases is multiple isomorphous replacement (MIR). For an object as large as ribosomal particles, it is necessary to use extremely dense and ultra-heavy compounds for derivatization. Examples of such compounds are tetrakis(acetoxy-mercuri)methane (TAMM) which was the key heavy-atom derivative in the structure determination of nucleosomes and the membrane reaction center [33,34], and an undecagold cluster, in which the gold core has a diameter of 8.2 Å (refs. [35,36] and fig. 8). Several variations of this cluster, modified with different ligands have been prepared (S. Weinstein and W. Jahn, in preparation). The cluster compounds in which all the moieties (R in fig. 8) are amine groups are soluble in the crystallization solution of 50S subunits from *H. marismortui* and were used for the formation of a heavy-atom derivative by soaking of native crystals in its solution. Crystallographic data (to 18 Å resolution) show isomorphous unit cell constants with observable differences in the intensities (fig. 7b).

Because the surface of the ribosomal subunit has a variety of potential binding sites for such clusters, in parallel to soaking experiments, at-

tempts to covalently bind heavy-atoms to a few specific sites on the ribosomal particles prior to crystallization are in progress. This may be achieved either by direct interaction of a heavy-atom cluster with chemically active groups such as -SH or the ends of rRNA [37] on the intact particles or by covalent attachment of a cluster to natural or tailor-made carriers which bind specifically to ribosomes.

The following approaches were taken: Firstly, free sulfhydryls on the surface of the 50S subunit have been located by reacting with radioactive N-ethylmaleimide. The labeled proteins were identified by locating radioactivity on two-dimensional electropherograms. It was found that in the case of 50S subunits from *B. stearothermophilus* there are mainly two proteins (BL11 and BL13) which bind N-ethylmaleimide. For *H. marismortui* a significant portion of the radioactivity was associated with a single protein. Secondly, the gold cluster described above was prepared such that it could be bound to accessible -SH groups. Since this cluster is rather bulky, its accessibility was increased by the insertion of spacers, differing in length, to the cluster as well as to the free -SH groups on the ribosomal particles. Radioactive labelling of this cluster as well as neutron activa-

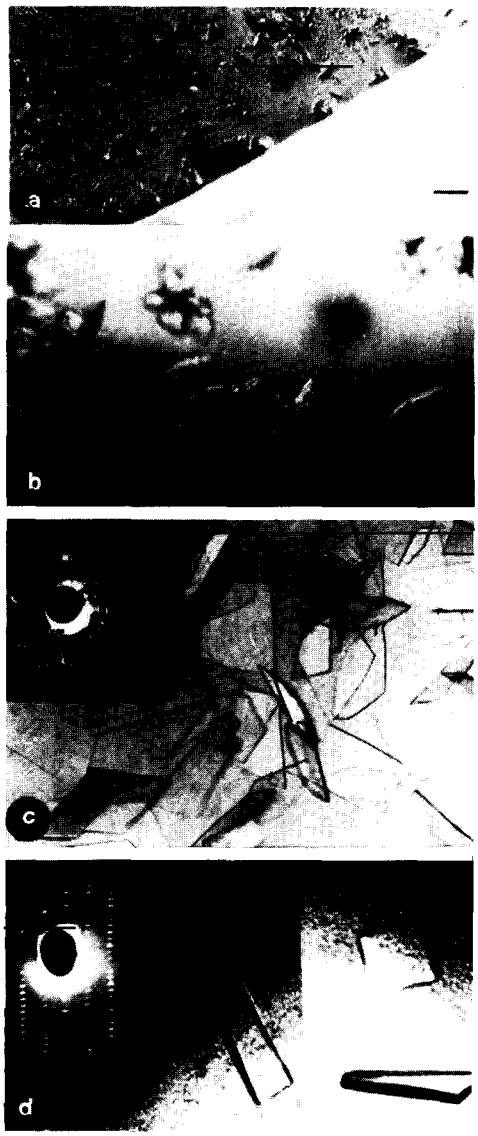

Fig. 6. Growth of large, ordered three-dimensional crystals of the 50S ribosomal subunits from *Halobacterium marismortui* by vapor diffusion at 19 °C (bar = 0.2 mm). (a) Microcrystals obtained within 1–2 days. Droplets of 7–8% polyethylene glycol (PEG), 2.5M KCl, 0.5M ammonium chloride, 0.15–0.20M magnesium chloride and 10mM spermidine, pH 5.0–5.2, were equilibrated with 3.0M KCl, 9% polyethylene glycol, 0.5M ammonium chloride and 0.20M magnesium chloride. (b) Crystals obtained within 2–3 days in droplets containing lower KCl concentration than used in (a). Droplet of 4–5% polyethylene glycol, 1.2–1.7M KCl, 0.5M ammonium chloride, 0.10M magnesium chloride and 10mM spermidine were equilibrated with reservoirs as in (a). (c) Crystals obtained within 3–5 days from droplets similar to those used for (b), equilibrated with reservoirs of lower KCl concentrations. Droplets of 4–5% polyethylene glycol, 1.2M KCl, 0.5M ammonium chloride, 0.05–0.10M magnesium chloride and 10mM spermidine, pH 5.0–5.6, were equilibrated with 1.7M KCl, 9% polyethylene glycol, 0.5M ammonium chloride and 0.10M magnesium chloride. An X-ray diffraction pattern taken perpendicular to the thin axis of the crystals obtained under conditions similar to those described in fig. 7 is inserted. (d) Crystals obtained by seeding of crystals from (c) in a crystallization drop containing 5% polyethylene glycol, 1.2M KCl, 0.5M ammonium chloride, 0.03M magnesium chloride, at pH 5.6, which was equilibrated with 7% PEG, 1.7M KCl, 0.5M ammonium chloride and 0.03M magnesium chloride, pH 5.6. Seeds were small and well-shaped crystals transferred into a stabilization solution of 7% polyethylene glycol in 1.7M KCl, 0.5M ammonium chloride, and 0.05M magnesium chloride at pH 5.6. An X-ray diffraction pattern taken perpendicular to the thin axis of the crystals obtained under conditions described in fig. 7 is inserted.

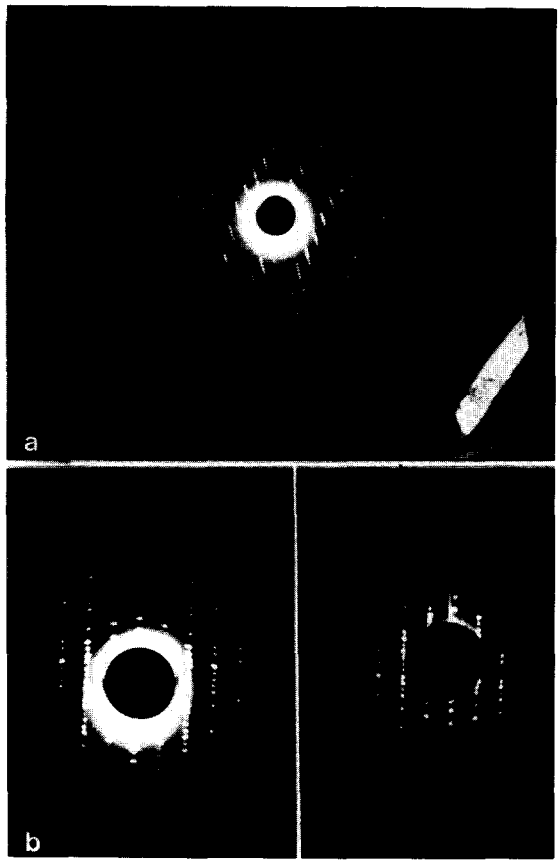

Fig. 7. (a) A 1° rotation pattern of a crystal similar to the inserted one. The pattern was obtained after 6 h of irradiation at −180°C with synchrotron X-ray beam (7.1 station at SSRL/Stanford University). Wave length: 1.54 Å. Exposure time: 2 min. Crystal-to-film distance: 135 mm. Insert: A crystal grown under the condition of fig. 6d. (b) The inner parts of X-ray diffraction patterns of native crystals (left) and of soaked crystals in a solution of the gold cluster (see fig. 8), obtained as in (a).

tion analysis of the gold element enabled us to determine the extent of binding of the cluster to the particles. The results of both analytical methods show that a spacer of minimum length of about 10 Å between the –SH group of a ribosomal protein and the N-atom on the cluster is needed for significant binding. Preliminary experiments indicate that the products of the derivatization reaction with 50S particles can be crystallized.

As mentioned above, such clusters may also be bound to biochemical carriers. Examples for these are antibiotics [38], DNA oligomers complementary to exposed single-stranded rRNA regions [39] and Fab fragments of antibodiess specific to ribosomal proteins. Since most of the interactions of these compounds are characterized biochemically, the crystallographic location of the heavy-atom compounds will not only be used for phase determination but will also reveal the specific functional sites on the ribosome.

Alternatively, such clusters may be attached to selected sites on isolated ribosomal components which will subsequently be incorporated into particles lacking these particular components. A mutant of *B. stearothermophilus* which lacks protein BL11 was obtained by growing cells in the presence of thiostrepton at 50°C [40]. The 50S mutated ribosomal subunits crystallize in two and three dimensions under the conditions used for 50S ribosomal subunits of the wild type, and yield isomorphous crystals [12]. This indicates that BL11, the missing protein, is not involved in crystal forces in the native crystals. Furthermore, protein BL11 has only one sulfhydryl group, and binding of N-ethylmaleimide to it does not reduce the biological activity and crystallizability.

Since protein BL11 is nearly globular [41], its location may be determined in a Patterson map with coefficients of $[F(\text{wild}) - F(\text{mutant})]$ and may serve, by itself, as a giant heavy-atom derivative. At preliminary stages of structure determination this approach may provide phase information and reveal the location of the missing protein.

Along these lines we have adapted a procedure for depleting the 50S subunits from several selected proteins [42]. We were able to remove and identify six proteins: BL1, BL6, BL10, BL11, and BL12 and BL16. Several combinations of five of these proteins were added to the depleted particles, and the activity and crystallizability of the partially reconstituted particles were checked. Preliminary results of these studies reconfirm our previous observations regarding mutated ribosomes (missing BL11). Furthermore, we found that there is an agreement between the recovery of activity in the reconstituted particles and our ability to crystallize them. Thus, particles missing BL12 which lost their biological activity completely, could not be crystallized, whereas after BL12 was incorpo-

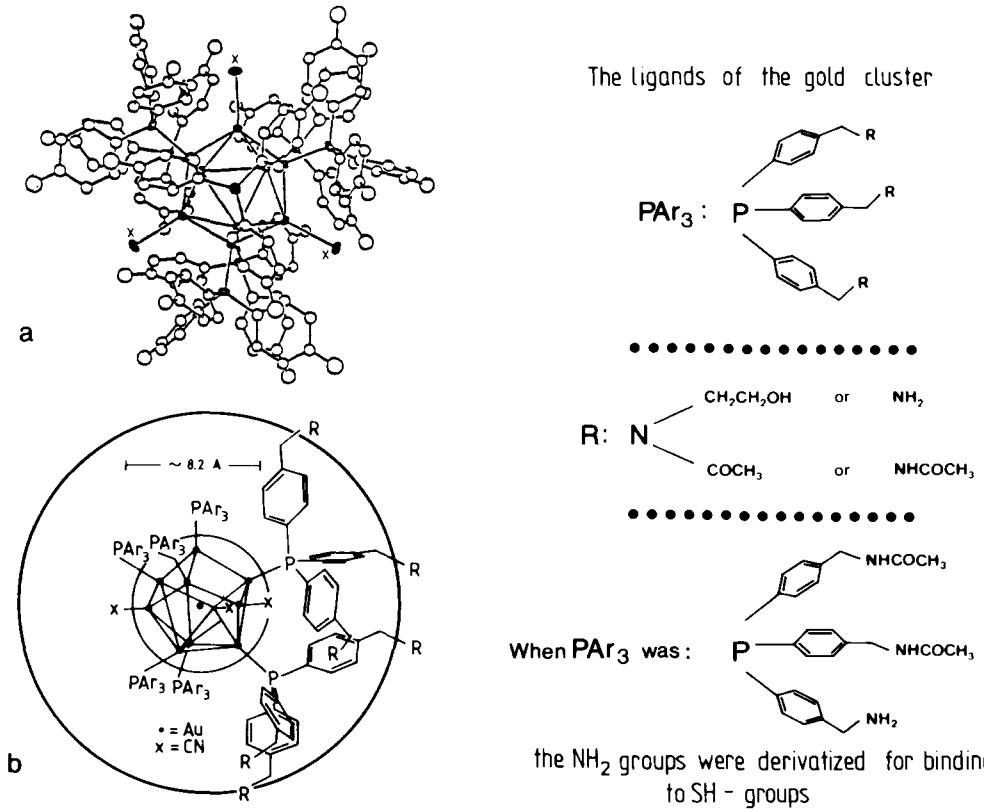

Fig. 8. (a) Postulated molecular structure of the gold cluster used by us based on the crystal structure of a similar cluster. (b) Semi-schematic presentation of the gold cluster depicting the gold core of 8.2 Å diameter and the arrangement of the ligands around it.

rated, the biological activity was regained and the reconstituted particles produced crystals isomorphous with the native form.

3.2. Three-dimensional image reconstruction

The large size of ribosomal particles which is an obstacle for crystallographic studies permits direct investigation by electron microscopy. Images of crystalline ribosomal particles may show the location and orientation of the particles within the crystals. A model obtained by three-dimensional image reconstruction of two-dimensional sheets may be used for gradual phasing of low resolution crystallographic data. To this end, we have initiated three-dimensional image reconstruction studies.

Two-dimensional sheets from prokaryotic ribosomal subunits have at first been grown in vitro from low molecular weight alcohols by vapor diffusion in hanging drops [14,43]. Recently, we have developed a procedure for obtaining two-dimensional sheets from mixtures of salts and alcohols within a few seconds [7,8,21,22].

Well ordered two-dimensional sheets from the 70S ribosomes and from 50S ribosomal subunits from *B. stearothermophilus* have been subjected to three-dimensional image reconstruction studies at 47 and 30 Å resolution, respectively [8,21]. In both cases the reconstructed particles have dimensions similar to those determined by other physical methods [3].

On the basis of the known molecular weight of these particle and of the volume obtained from the

three-dimensional image reconstruction, the calculated densities are in good agreement with values tabulated [44] and calculated for the crystals of the 50S subunits from *H. marismortui* [17] and other nucleoproteins [45,46].

3.2.1. Two-dimensional sheets of 70S ribosomes

The two-dimensional sheets of 70S particles from *Bacillus stearothermophilus* are built of dimers, packed in relatively small unit cells (about 192×420Å). Analysis of the models obtained by three-dimensional reconstruction of sheets stained with gold-thioglucose show that the two ribosomal subunits are arranged around an empty space, large enough to accommodate components of protein biosynthesis, e.g. tRNAs, elongation factors, etc. [8]. There is a similarity between the model of the small subunit obtained by visualization of single particles [3] and that revealed by our studies. However, isolated 30S particles appear somewhat wider than those reconstructed within the 70S particles. This may be a consequence of the contact of the isolated particles with the flat electron microscope grid. In contrast, particles within the crystalline sheets are held together by crystalline forces. These form a network which may stabilize the conformation of the particle and diminish or even eliminate the influence of the flatness of the grids. The portion of the reconstructed 70S particle which we assigned as the large subunit may be correlated to the image of this subunit as reconstructed from sheets of 50S particles (fig. 9 and ref. [21]).

Reconstruction from sheets of 70S ribosomes stained with uranyl acetate led to a model which shows the features described above as well as regions where uranyl acetate, acting as a positive stain, was incorporated into the particle. This may indicate that in these regions the RNA, the natural candidate for these interactions, is concentrated and exposed to the stain. Such regions are located on the body of the small subunit and on the interface of the small and the large subunit, in good agreement with previous studies [47].

3.2.2. Two-dimensional sheets of 50S ribosomal subunits

Two-dimensional sheets of 50S subunits consist of small unit cells, $(140 \pm 20) \times (330 \pm 20)$ Å, close to those of forms #1 and #2 of the three-dimensional crystals from the same source [14,21,48]. Optical diffraction patterns of electron micrographs of specimens negatively stained with gold-thioglucose extend to about 30 Å (fig. 10). Three-dimensional image reconstruction of these sheets yielded a model which shows several projecting arms, two of which are longer than the others. They are arranged radially around one edge near the presumed interface with the 30S subunit. A narrow elongated cleft is formed between the projecting arms and turns into a tunnel of a diameter of up to 25 Å and 100–120 Å length (fig. 10). A similar feature was also detected on ribosomes from chick embryos by three-dimensional image reconstruction [47].

The functional significance of the tunnel is still to be determined. However, originating at the presumed site of actual protein biosynthesis, terminating on the other end of the particle, and being wide enough to accommodate even the bulkiest amino acid and of a length compatible with a peptide of about 40 amino acids, this tunnel appears to provide the path taken by the nascent polypeptide chain. It was found biochemically that the ribosomes protect newly synthesized peptides of about 30–40 amino acids from proteolytic enzymes [49–51]. It remains to be seen whether the tunnel terminates at a location compatible with that assigned by immune electron microscopy as the exit site for the growing polypeptide chain [52].

Thirteen reconstructed models of the 50S particles were examined. The tunnel is revealed in all reconstructions independent of the staining material (gold thioglucose or uranyl acetate). In every reconstructed particle there is a region of low density which branches off the tunnel to form a Y (or V) shape and terminates on the opposite side of the particle (fig. 10). As yet the exact nature of this region cannot be determined. It may be a loosely packed protein regions, but in some reconstructed models the density of this region is so low that it appears as a branch of the main tunnel.

Several models for 50S ribosomal subunits of *E.* coli have been suggested, based on electron microscopial visualization, reconstruction or aver-

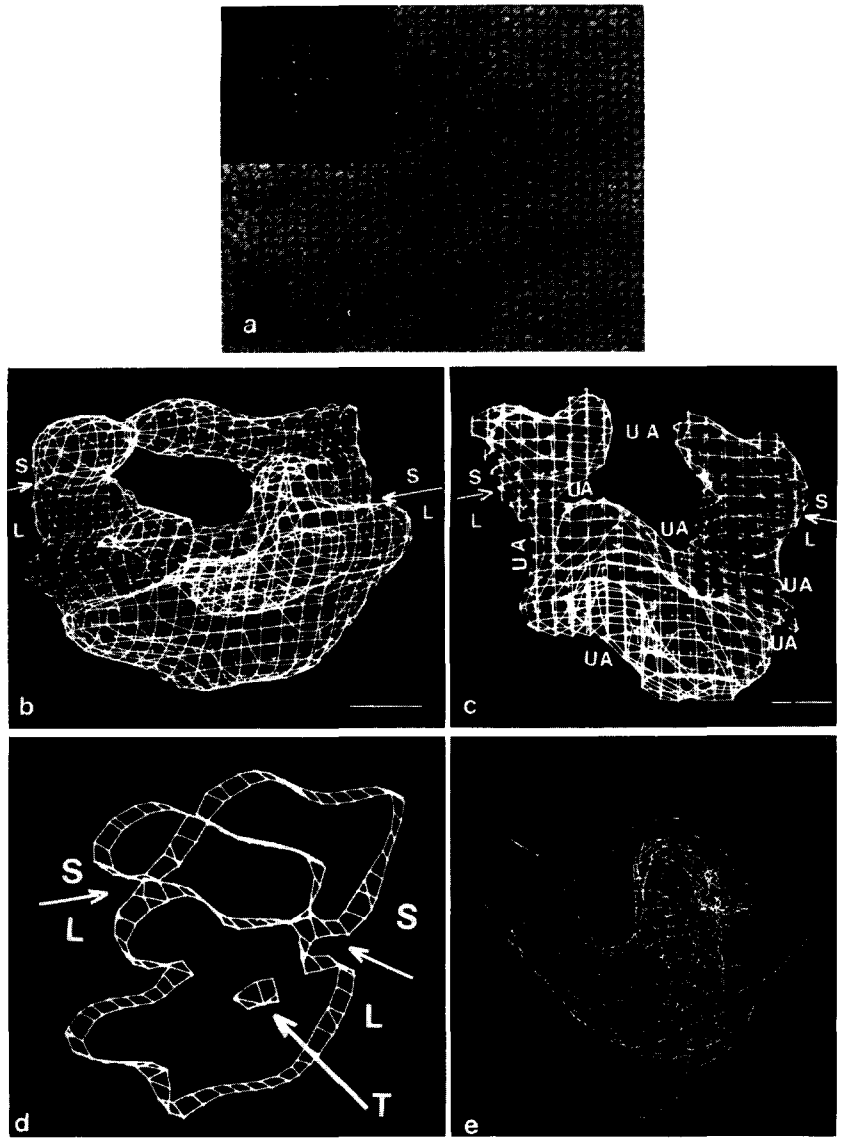

Fig. 9. (a) An image of a two-dimensional sheet (×28000) of 70S particles from *B. stearothermophilus* stained with gold-thioglucose, and an optical diffraction pattern from an area containing about 20×15 unit cells. (b) Computer graphic display of the outline of the reconstructed model of the 70S ribosome at 47 å resolution stained with gold-thioglucose. L and S indicate the 50S and the 30S subunits, respectively. The arrows point at the interface between the two subunits (bar = 20 Å). (c) Computer graphic display of the outline of the reconstructed model of the 70S ribosome at 42 Å resolution stained with uranyl acetate, at a similar orientation to that shown in (b). UA shows the regions to which uranyl acetate binds. L and S indicate the 50S and the 30S subunits, respectively. The arrows point at the interface between the two subunits. Bar length = 20 Å. (d) Outline of a 20 Å thick section in the middle of the reconstructed model of the 70S ribosome. T indicates part of the tunnel. (e) Computer graphic display of the reconstructed model of the 50S subunit at 30 Å resolution, obtained as in fig. 10 and viewed in a projection which resembles models derived from electron microscopy studies of single particles.

aging of single particles [3]. Our model can be positioned in such a way that its projected view resembles that usual image seen when single particles are investigated by electron microscopy (fig. 9). However, there are major discrepancies in the nature of the gross structural features between our

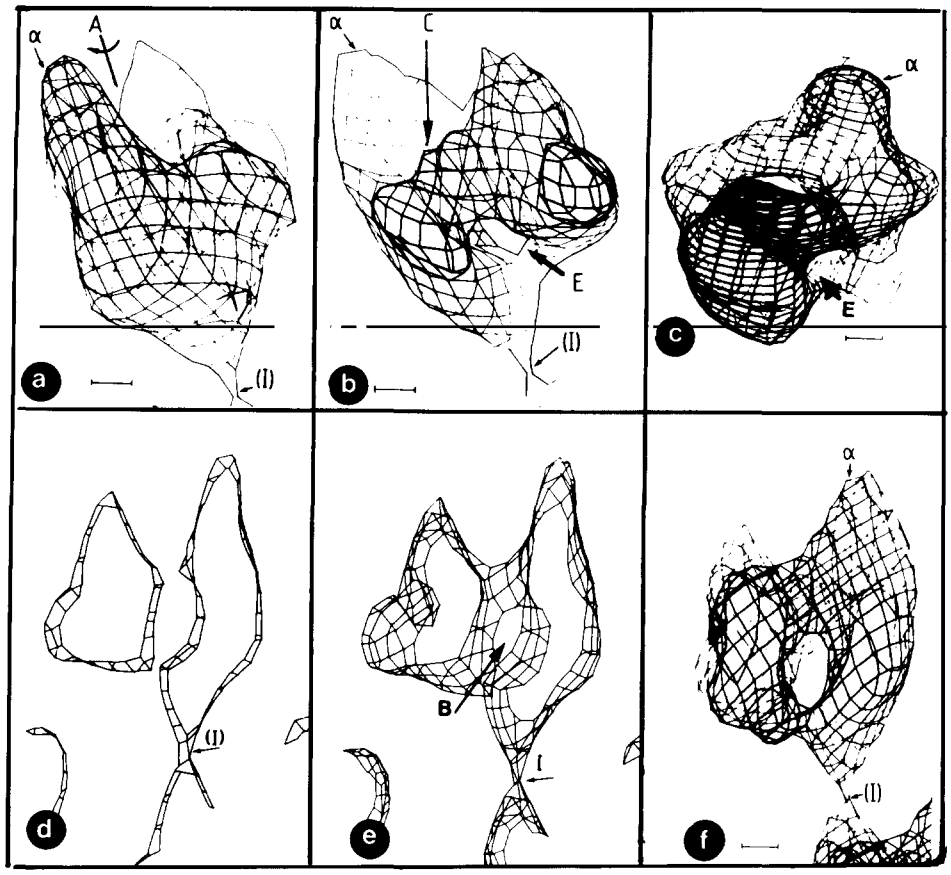

Fig. 10. Computer graphic display of the reconstructed model of the 50S ribosomal subunits at 30 Å resolution. α marks the longest arm. (E) is the exit site. (a) A side view of the model. The entire particle and part of a second one are shown. The arrow (I) points at the crystal contact between the two particles. (A) marks the approximate axis around which the model was turned to obtain the view shown in (b) (bar = 20 Å). (b) The model shown in (a) rotated about the (A) axis. (C) points at the cleft between the projecting arms, at the site it turns into the tunnel. (c) A view into the tunnel from the cleft. (d) Outline of a 20 Å thick section in the middle of the reconstructed model, showing that the tunnel spans through the particle. (e) Outline of a 40 Å thick section in the middle of the reconstructed model. The branching of the tunnel is seen (B). (f) Model viewed into the branch of the tunnel from the exit point.

model and the others. These, as in the case of the 70S particles, may stem from the basic differences between subjective visualization of isolated particles in projection on the one hand, and the inherently more objective character of structure analysis by diffraction methods on the other hand.

In the reconstructed 70S ribosomes from B. stearothermophilus there are also some indications for the existence of a tunnel. Thus, portions of the tunnel could be detected in 20–40 Å thick sections through the particle. An example is shown in fig. 9. Since the 70S particles used for these studies were harvested while being active, it is feasible that they contain nascent protein chains. This may be the reason for the fact that the tunnel is only partially resolved.

4. Concluding remarks

We have demonstrated here that crystallographic studies may be carried out on intact ribosomal particles. We expect that these studies, supported by electron microscopy and combined with the available biophysical, biochemical and genetic knowledge, will yield a reliable model for the

ribosome and contribute to the understanding of the molecular mechanism of protein biosynthesis.

Acknowledgements

We would like to thank Dr. H. Hope for introducing cryo-temperature crystallography; Drs. M.A. Saper, K.S. Bartels, C. Kratky and G. Weber for their efforts in data collection; Dr. K.R. Leonard and T. Arad for their contribution to the image reconstruction studies; Dr. F.L. Hirshfeld for his critical comments; Drs. J. Sussman and B. Shaanan for assisting us with computing and display problems; Drs. K. Wilson, H.D. Bartunik, J. Helliwell, M. Papiz, K. Moffat, W. Schildcamp, P. Pizackerley, and E. Merrit in providing synchrotron radiation facilities; and P. Webster, H.S. Gewitz, J. Piefke, Y. Halfon, B. Romberg, G. Idan and H. Danz for technical assistance.

This work was supported by BMFT (05 180 MP B0), NIH (GM 34360) and Minerva research grants.

References

[1] G. Chambliss, G.R. Craven, J. Davies, L. Kahan and M. Nomura, Eds., Ribosomes: Structure, Function and Genetics (University Park Press, Baltimore, MD, 1980).
[2] H.G. Wittmann, Ann. Rev. Biochem. 51 (1982) 155.
[3] H.G. Wittmann, Ann. Rev. Biochem. 52 (1983) 35.
[4] B. Hardesty and G. Kramer, Eds., Structure, Function and Genetics of Ribosomes (Springer, Berlin, 1986).
[5] A. Yonath, J. Müssig and H.G. Wittmann, J. Cell Biochem. 19 (1982) 145.
[6] H.G. Wittmann, J. Müssig, H.S. Gewitz, J. Piefke, H.J. Rheinberger and A. Yonath, FEBS Letters 146 (1982) 217.
[7] J. Piefke, T. Arad, I. Makowski, H.S. Gewitz, B. Hennemann, A. Yonath and H.G. Wittmann, FEBS Letters 209 (1986) 104.
[8] T. Arad, J. Piefke, S. Weinstein, H.S. Gewitz, A. Yonath and H.G. Wittmann, Biochimie 69 (1987) 1001.
[9] A. Yonath, J. Müssig, B. Tesche, S. Lorenz, V.A. Erdmann and H.G. Wittmann, Biochem. Intern. 1 (1980) 428.
[10] A. Yonath, H.D. Bartunik, K.S. Bartels and H.G. Wittmann, J. Mol. Biol. 177 (1984) 201.
[11] A. Yonath, M.A. Saper, I. Makowski, J. Müssig, J. Piefke, H.D. Bartunik, K.S. Bartels and H.G. Wittmann, J. Mol. Biol. 187 (1986) 633.
[12] A. Yonath, M.A. Saper, F. Frolow, I. Makowski and H.G. Wittmann, J. Mol. Biol. 192 (1986) 161.
[13] C. Glotz, J. Müssig, H.S. Gewitz, I. Makowski, T. Arad, A. Yonath, and H.G. Wittmann, Biochem. Intern. 15 (1987) 953.
[14] T. Arad, K.R. Leonard, H.G. Wittmann and A. Yonath, EMBO J. 3 (1984) 127.
[15] A. Shevack, A., H.S. Gewitz, B. Hennemann, A. Yonath and H.G. Wittmann, FEBS Letters 184 (1985) 68.
[16] M. Shoham, M., J. Müssig, A. Shevack, T. Arad, H.G. Wittmann and A. Yonath, FEBS Letters 208 (1986) 321.
[17] I. Makowski, F. Frolow, M.A. Saper, H.G. Wittmann and A. Yonath, J. Mol. Biol. 193 (1987) 819.
[18] A. Yonath and H.G. Wittmann. in: Methods in Enzymology, Vol. 164, Eds. K. Moldave and H. Noller (Academic Press, Orlando, FL, 1988).
[19] A. Yonath, K.R. Leonard, S. Weinstein and H.G. Wittmann, Spring Harbor Symp., 1988, in press.
[20] A. Yonath and H.G. Wittmann, in: Proc. 5th Albany Conversation, 1988, Ed. M. Sarma, in press.
[21] A. Yonath, K.R. Leonard and H.G. Wittmann, Science 236 (1987) 813.
[22] T. Arad, J. Piefke, H.S. Gewitz, B. Romberg, C. Glotz, J. Müssig, A. Yonath and H.G. Wittmann, Anal. Biochem. 167 (1987) 113.
[23] P.A. Bartlett, B. Bauer and S.J. Singer, J. Am. Chem. Soc. 100 (1978) 5085.
[24] A. Yonath, G. Khavitch, B. Tesche, J. Müssig, S. Lorenz, V.A. Erdmann and H.G. Wittmann, Biochem. Intern. 5 (1982) 629.
[25] A. Klug, K.C. Holmes and J.T. Finch, J. Mol. Biol. 3 (1961) 87.
[26] G. Zubay and M.H.F. Wilkins, J. Mol. Biol. 2 (1960) 105.
[27] R. Langridge and K.C. Holmes, J. Mol Biol. 5 (1962) 611.
[28] J.T. Finch, L.C. Lutter, D. Rhodes, R.S. Brown, B. Rushton, M. Levitt and A. Klug, Nature 269 (1977) 29.
[29] M.G. Rossmann and W. Erickson, J. Appl. Cryst. 16 (1983) 629.
[30] J.W. Gibbs, in: Collected Works of J.W. Gibbs (Longmans, Green and Co., London, 1928) pp. 55–70.
[31] A.C. Zettlemoyer, Nucleation (Dekker, New York, 1969).
[32] Z. Kam, H.B. Shore and G. Fehder, J. Mol. Biol. 123 (1978) 539.
[33] J. Deisenhofer, O. Epp, K. Mikki, R. Huber and H. Michel, J. Mol. Biol. 180 (1984) 385.
[34] T. Richmond, J.T. Finch, B. Rushton, D. Rhodes and A. Klug, Nature 311 (1984) 533.
[35] P. Bellon, P.M. Manassero and M. Sansoni, J. Chem. Soc. Dalton Trans. (1972) 1481.
[36] J.S. Wall, J.F. Hainfeld, P.A. Barlett and S.J. Singer, Ultramicroscopy 8 (1982) 397.
[37] O.W. Odom, Jr., D.R. Robbins, J. Lynch, D. Dottavio-Martin, G. Kramer and B. Hardesty, Biochemistry 19 (1980) 5941.
[38] K.H. Nierhaus and H.G. Wittmann, Naturwissenschaften 67 (1980) 234.
[39] W.E. Hill, B.E. Trappich and B. Tassanakajohn, in: Structure, Function and Genetics of Ribosomes, Eds. B. Hardesty and G. Kramer (Springer, Berlin 1986) pp. 233–252.

[40] J. Schnier, H.S. Gewitz and B. Leighton, manuscript in preparation.
[41] L. Giri, W.E. Hill, H.G. Wittmann and B. Wittmann-Liebold, Advan. Protein Chem. 36 (1984) 1.
[42] H.S. Gewitz, C. Glotz, P. Goischke, B. Romberg, A. Yonath and H.G. Wittmann, Biochem. Intern. 15 (1987) 887.
[43] M.W. Clark, K.R. Leonard and J.A. Lake, Science 216 (1982) 999.
[44] B.W. Matthews, J. Mol. Biol. 33 (1968) 491.
[45] J.M. Hogle, J. Mol. Biol. 160 (1982) 663.
[46] L. Liljas, T. Unge, A. Jones, K. Fridborg, S. Lovgren, U. Skoglund and B. Strandberg, J. Mol. Biol. 159 (1982) 93.
[47] R.A. Milligan and P.N.T. Unwin, Nature 319 (1986) 693.
[48] A. Yonath, Trends Biochem. Sci. 9 (1984) 227.
[49] L.I. Malkin and A. Rich, J. Mol. Biol. 26 (1967) 329.
[50] G. Blobel and D.D. Sabatini, J. Cell. Biol. 45 (1970) 130.
[51] W.P. Smith, P.C. Tai and B.D. Davis, Proc. Natl. Acad. Sci. USA 75 (1978) 5922.
[52] C. Bernabeau and J.A. Lake, Proc. Natl. Acad. Sci. USA 79 (1982) 3111.